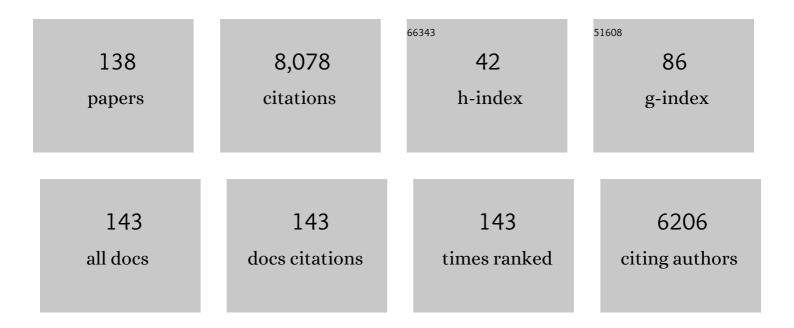
List of Publications by Year in descending order

Source: https://exaly.com/author-pdf/7764133/publications.pdf Version: 2024-02-01



KENSLIKE TONO

#	Article	IF	CITATIONS
1	A compact X-ray free-electron laser emitting in the sub-ångström region. Nature Photonics, 2012, 6, 540-544.	31.4	1,542
2	Light-induced structural changes and the site of O=O bond formation in PSII caught by XFEL. Nature, 2017, 543, 131-135.	27.8	515
3	A three-dimensional movie of structural changes in bacteriorhodopsin. Science, 2016, 354, 1552-1557.	12.6	350
4	An oxyl/oxo mechanism for oxygen-oxygen coupling in PSII revealed by an x-ray free-electron laser. Science, 2019, 366, 334-338.	12.6	248
5	Determination of damage-free crystal structure of an X-ray–sensitive protein using an XFEL. Nature Methods, 2014, 11, 734-736.	19.0	237
6	Focusing of X-ray free-electron laser pulses with reflective optics. Nature Photonics, 2013, 7, 43-47.	31.4	234
7	Beamline, experimental stations and photon beam diagnostics for the hard x-ray free electron laser of SACLA. New Journal of Physics, 2013, 15, 083035.	2.9	230
8	Direct observation of bond formation in solution with femtosecond X-ray scattering. Nature, 2015, 518, 385-389.	27.8	207
9	Grease matrix as a versatile carrier of proteins for serial crystallography. Nature Methods, 2015, 12, 61-63.	19.0	193
10	Imaging live cell in micro-liquid enclosure by X-ray laser diffraction. Nature Communications, 2014, 5, 3052.	12.8	183
11	Two-colour hard X-ray free-electron laser with wide tunability. Nature Communications, 2013, 4, 2919.	12.8	172
12	Determination of the Pulse Duration of an X-Ray Free Electron Laser Using Highly Resolved Single-Shot Spectra. Physical Review Letters, 2012, 109, 144801.	7.8	162
13	Untangling the sequence of events during the S <sub>2</sub> → S <sub>3</sub> transition in photosystem II and implications for the water oxidation mechanism. Proceedings of the National Academy of Sciences of the United States of America, 2020, 117, 12624-12635.	7.1	149
14	Deep Inner-Shell Multiphoton Ionization by Intense X-Ray Free-Electron Laser Pulses. Physical Review Letters, 2013, 110, 173005.	7.8	136
15	Generation of 1020 W cmâ^'2 hard X-ray laser pulses with two-stage reflective focusing system. Nature Communications, 2014, 5, 3539.	12.8	124
16	X-Ray Second Harmonic Generation. Physical Review Letters, 2014, 112, 163901.	7.8	116
17	Single-shot beam-position monitor for x-ray free electron laser. Review of Scientific Instruments, 2011, 82, 023108.	1.3	94
18	Generation of narrow-band X-ray free-electron laser via reflection self-seeding. Nature Photonics, 2019, 13, 319-322.	31.4	81

#	Article	IF	CITATIONS
19	Diverse application platform for hard X-ray diffraction in SACLA (DAPHNIS): application toÂserial protein crystallography using an X-ray free-electron laser. Journal of Synchrotron Radiation, 2015, 22, 532-537.	2.4	80
20	Observation of femtosecond X-ray interactions with matter using an X-ray–X-ray pump–probe scheme. Proceedings of the National Academy of Sciences of the United States of America, 2016, 113, 1492-1497.	7.1	80
21	A soft X-ray free-electron laser beamline at SACLA: the light source, photon beamline and experimental station. Journal of Synchrotron Radiation, 2018, 25, 282-288.	2.4	78
22	Data processing pipeline for serial femtosecond crystallography at SACLA. Journal of Applied Crystallography, 2016, 49, 1035-1041.	4.5	76
23	Hydroxyethyl cellulose matrix applied to serial crystallography. Scientific Reports, 2017, 7, 703.	3.3	74
24	Capturing an initial intermediate during the P450nor enzymatic reaction using time-resolved XFEL crystallography and caged-substrate. Nature Communications, 2017, 8, 1585.	12.8	74
25	Single Shot Coherence Properties of the Free-Electron Laser SACLA in the Hard X-ray Regime. Scientific Reports, 2014, 4, 5234.	3.3	69
26	A nanosecond time-resolved XFEL analysis of structural changes associated with CO release from cytochrome c oxidase. Science Advances, 2017, 3, e1603042.	10.3	68
27	Dose-resolved serial synchrotron and XFEL structures of radiation-sensitive metalloproteins. IUCrJ, 2019, 6, 543-551.	2.2	65
28	XFEL structures of the influenza M2 proton channel: Room temperature water networks and insights into proton conduction. Proceedings of the National Academy of Sciences of the United States of America, 2017, 114, 13357-13362.	7.1	64
29	Macromolecular structures probed by combining single-shot free-electron laser diffraction with synchrotron coherent X-ray imaging. Nature Communications, 2014, 5, 3798.	12.8	61
30	Nanoplasma Formation by High Intensity Hard X-rays. Scientific Reports, 2015, 5, 10977.	3.3	60
31	Photoswitching mechanism of a fluorescent protein revealed by time-resolved crystallography and transient absorption spectroscopy. Nature Communications, 2020, 11, 741.	12.8	56
32	Double Core-Hole Creation by Sequential Attosecond Photoionization. Physical Review Letters, 2013, 111, 043001.	7.8	55
33	A Bragg beam splitter for hard x-ray free-electron lasers. Optics Express, 2013, 21, 2823.	3.4	55
34	Crystal Structures of Human Orexin 2 Receptor Bound to the Subtype-Selective Antagonist EMPA. Structure, 2018, 26, 7-19.e5.	3.3	55
35	An isomorphous replacement method for efficient de novo phasing for serial femtosecond crystallography. Scientific Reports, 2015, 5, 14017.	3.3	54
36	Toward G protein-coupled receptor structure-based drug design using X-ray lasers. IUCrJ, 2019, 6, 1106-1119.	2.2	53

#	Article	IF	CITATIONS
37	Wavelength-tunable split-and-delay optical system for hard X-ray free-electron lasers. Optics Express, 2016, 24, 9187.	3.4	52
38	Native sulfur/chlorine SAD phasing for serial femtosecond crystallography. Acta Crystallographica Section D: Biological Crystallography, 2015, 71, 2519-2525.	2.5	51
39	Crystallography on a chip – without the chip: sheet-on-sheet sandwich. Acta Crystallographica Section D: Structural Biology, 2018, 74, 1000-1007.	2.3	51
40	Multiple application X-ray imaging chamber for single-shot diffraction experiments with femtosecond X-ray laser pulses. Journal of Applied Crystallography, 2014, 47, 188-197.	4.5	49
41	Structure of the dopamine D2 receptor in complex with the antipsychotic drug spiperone. Nature Communications, 2020, 11, 6442.	12.8	47
42	Oil-free hyaluronic acid matrix for serial femtosecond crystallography. Scientific Reports, 2016, 6, 24484.	3.3	46
43	3D visualization of XFEL beam focusing properties using LiF crystal X-ray detector. Scientific Reports, 2016, 5, 17713.	3.3	43
44	Membrane protein structure determination by SAD, SIR, or SIRAS phasing in serial femtosecond crystallography using an iododetergent. Proceedings of the National Academy of Sciences of the United States of America, 2016, 113, 13039-13044.	7.1	43
45	Nanofocusing of X-ray free-electron laser using wavefront-corrected multilayer focusing mirrors. Scientific Reports, 2018, 8, 17440.	3.3	43
46	Direct observation of picosecond melting and disintegration of metallic nanoparticles. Nature Communications, 2019, 10, 2411.	12.8	43
47	High-viscosity sample-injection device for serial femtosecond crystallography at atmospheric pressure. Journal of Applied Crystallography, 2019, 52, 1280-1288.	4.5	43
48	High-Resolution XFEL Structure of the Soluble Methane Monooxygenase Hydroxylase Complex with its Regulatory Component at Ambient Temperature in Two Oxidation States. Journal of the American Chemical Society, 2020, 142, 14249-14266.	13.7	41
49	Time-resolved serial femtosecond crystallography reveals early structural changes in channelrhodopsin. ELife, 2021, 10, .	6.0	41
50	Dynamic fracture of tantalum under extreme tensile stress. Science Advances, 2017, 3, e1602705.	10.3	41
51	Superradiance of an ensemble of nuclei excited by a free electron laser. Nature Physics, 2018, 14, 261-264.	16.7	39
52	High-throughput structures of protein–ligand complexes at room temperature using serial femtosecond crystallography. IUCrJ, 2019, 6, 1074-1085.	2.2	36
53	Serial femtosecond crystallography structure of cytochrome c oxidase at room temperature. Scientific Reports, 2017, 7, 4518.	3.3	34
54	Structural basis for light control of cell development revealed by crystal structures of a myxobacterial phytochrome. IUCrJ, 2018, 5, 619-634.	2.2	33

#	Article	IF	CITATIONS
55	Multiple-beamline operation of SACLA. Journal of Synchrotron Radiation, 2019, 26, 595-602.	2.4	32
56	Characterization of temporal coherence of hard X-ray free-electron laser pulses with single-shot interferograms. IUCrJ, 2017, 4, 728-733.	2.2	32
57	Comparing serial X-ray crystallography and microcrystal electron diffraction (MicroED) as methods for routine structure determination from small macromolecular crystals. IUCrJ, 2020, 7, 306-323.	2.2	32
58	Measurement of the X-ray Spectrum of a Free Electron Laser with a Wide-Range High-Resolution Single-Shot Spectrometer. Applied Sciences (Switzerland), 2017, 7, 584.	2.5	31
59	High-resolution crystal structures of transient intermediates in the phytochrome photocycle. Structure, 2021, 29, 743-754.e4.	3.3	31
60	Status of the SACLA Facility. Applied Sciences (Switzerland), 2017, 7, 604.	2.5	29
61	Element Selectivity in Second-Harmonic Generation of <mml:math xmlns:mml="http://www.w3.org/1998/Math/MathML" display="inline"&gt;<mml:mrow><mml:msub><mml:mrow><mml:mi>GaFeO</mml:mi></mml:mrow><mml:mrow>&lt; by a Soft-X-Ray Free-Electron Laser. Physical Review Letters. 2018. 120. 223902.</mml:mrow></mml:msub></mml:mrow></mml:math 	m <b>7:8</b> :mn>3	3< <b>7</b> mml:mr⊳
62	Multi-wavelength anomalous diffraction de novo phasing using a two-colour X-ray free-electron laser with wide tunability. Nature Communications, 2017, 8, 1170.	12.8	28
63	Nanosecond pump–probe device for time-resolved serial femtosecond crystallography developed at SACLA. Journal of Synchrotron Radiation, 2017, 24, 1086-1091.	2.4	28
64	Superfluorescence, Free-Induction Decay, and Four-Wave Mixing: Propagation of Free-Electron Laser Pulses through a Dense Sample of Helium Ions. Physical Review Letters, 2018, 121, 263201.	7.8	27
65	X-ray Hanbury Brown-Twiss interferometry for determination of ultrashort electron-bunch duration. Physical Review Accelerators and Beams, 2018, 21, .	1.6	27
66	Redox-coupled structural changes in nitrite reductase revealed by serial femtosecond and microfocus crystallography. Journal of Biochemistry, 2016, 159, 527-538.	1.7	26
67	Damage threshold of coating materials on x-ray mirror for x-ray free electron laser. Review of Scientific Instruments, 2016, 87, 051801.	1.3	25
68	Performance of a hard X-ray split-and-delay optical system with a wavefront division. Journal of Synchrotron Radiation, 2018, 25, 20-25.	2.4	25
69	Necessary Experimental Conditions for Single-Shot Diffraction Imaging of DNA-Based Structures with X-ray Free-Electron Lasers. ACS Nano, 2018, 12, 7509-7518.	14.6	24
70	Capturing structural changes of the S <sub>1</sub> to S <sub>2</sub> transition of photosystem II using time-resolved serial femtosecond crystallography. IUCrJ, 2021, 8, 431-443.	2.2	24
71	Experimental phase determination with selenomethionine or mercury-derivatization in serial femtosecond crystallography. IUCrJ, 2017, 4, 639-647.	2.2	24
72	Serial crystallography captures dynamic control of sequential electron and proton transfer events in a flavoenzyme. Nature Chemistry, 2022, 14, 677-685.	13.6	24

#	Article	IF	CITATIONS
73	X-ray free-electron laser studies reveal correlated motion during isopenicillin <i>N</i> synthase catalysis. Science Advances, 2021, 7, .	10.3	23
74	Intense sub-micrometre focusing of soft X-ray free-electron laser beyond 1016 Wâ€cmâ^'2 with an ellipsoidal mirror. Journal of Synchrotron Radiation, 2019, 26, 1406-1411.	2.4	23
75	Single-pulse enhanced coherent diffraction imaging of bacteria with an X-ray free-electron laser. Scientific Reports, 2016, 6, 34008.	3.3	22
76	Angular correlations of photons from solution diffraction at a free-electron laser encode molecular structure. IUCrJ, 2016, 3, 420-429.	2.2	20
77	Beamline mirrors and monochromator for X-ray free electron laser of SACLA. Nuclear Instruments and Methods in Physics Research, Section A: Accelerators, Spectrometers, Detectors and Associated Equipment, 2013, 710, 139-142.	1.6	19
78	Time-interleaved multienergy acceleration for an x-ray free-electron laser facility. Physical Review Special Topics: Accelerators and Beams, 2013, 16, .	1.8	19
79	High-resolution crystal structures of a myxobacterial phytochrome at cryo and room temperatures. Structural Dynamics, 2019, 6, 054701.	2.3	19
80	Radiation-Induced Chemical Dynamics in Ar Clusters Exposed to Strong X-Ray Pulses. Physical Review Letters, 2018, 120, 223201.	7.8	18
81	XFEL Crystal Structures of Peroxidase Compound II. Angewandte Chemie - International Edition, 2021, 60, 14578-14585.	13.8	18
82	Characterizing transverse coherence of an ultra-intense focused X-ray free-electron laser by an extended Young's experiment. IUCrJ, 2015, 2, 620-626.	2.2	18
83	Dynamics of soft nanoparticle suspensions at hard X-ray FEL sources below the radiation-damage threshold. IUCrJ, 2018, 5, 801-807.	2.2	18
84	Fixed target single-shot imaging of nanostructures using thin solid membranes at SACLA. Journal of Physics B: Atomic, Molecular and Optical Physics, 2016, 49, 034008.	1.5	17
85	Nanofocusing Optics for an X-Ray Free-Electron Laser Generating an Extreme Intensity of 100 EW/cm2 Using Total Reflection Mirrors. Applied Sciences (Switzerland), 2020, 10, 2611.	2.5	17
86	Extreme Ultraviolet Second Harmonic Generation Spectroscopy in a Polar Metal. Nano Letters, 2021, 21, 6095-6101.	9.1	17
87	Following the Birth of a Nanoplasma Produced by an Ultrashort Hard-X-Ray Laser in Xenon Clusters. Physical Review X, 2018, 8, .	8.9	16
88	Development of an Experimental Platform for Combinative Use of an XFEL and a High-Power Nanosecond Laser. Applied Sciences (Switzerland), 2020, 10, 2224.	2.5	16
89	Polarization-Resolved Extreme-Ultraviolet Second-Harmonic Generation from <mml:math xmlns:mml="http://www.w3.org/1998/Math/MathML" display="inline"&gt; <mml:mrow> <mml:msub> <mml:mrow> <mml:mi> LiNbO </mml:mi> </mml:mrow> <ml:mrow> &lt; Physical Review Letters, 2021, 127, 237402.</ml:mrow></mml:msub></mml:mrow></mml:math 	mmi:mn>3	3
90	Room-temperature calorimeter for x-ray free-electron lasers. Review of Scientific Instruments, 2015, 86, 093104.	1.3	14

#	Article	IF	CITATIONS
91	Development of speckle-free channel-cut crystal optics using plasma chemical vaporization machining for coherent x-ray applications. Review of Scientific Instruments, 2016, 87, 063118.	1.3	14
92	Ultrafast Structural Dynamics of Nanoparticles in Intense Laser Fields. Physical Review Letters, 2019, 123, 123201.	7.8	14
93	On the size of the secondary electron cloud in crystals irradiated by hard X-ray photons. European Physical Journal D, 2017, 71, 1.	1.3	13
94	Systematic-error-free wavefront measurement using an X-ray single-grating interferometer. Review of Scientific Instruments, 2018, 89, 043106.	1.3	13
95	Ultrafast anisotropic disordering in graphite driven by intense hard X-ray pulses. High Energy Density Physics, 2019, 32, 63-69.	1.5	13
96	Full-field microscope with twin Wolter mirrors for soft X-ray free-electron lasers. Optics Express, 2019, 27, 33889.	3.4	12
97	Conformational alterations in unidirectional ion transport of a light-driven chloride pump revealed using X-ray free electron lasers. Proceedings of the National Academy of Sciences of the United States of America, 2022, 119, .	7.1	11
98	Pump-Probe Time-Resolved Serial Femtosecond Crystallography at SACLA: Current Status and Data Collection Strategies. Applied Sciences (Switzerland), 2019, 9, 5505.	2.5	10
99	Slowing down of dynamics and orientational order preceding crystallization in hard-sphere systems. Science Advances, 2020, 6, .	10.3	10
100	Viscosity-adjustable grease matrices for serial nanocrystallography. Scientific Reports, 2020, 10, 1371.	3.3	10
101	Using Diffuse Scattering to Observe X-Ray-Driven Nonthermal Melting. Physical Review Letters, 2021, 126, 015703.	7.8	10
102	Development of ultrafast pump and probe experimental system at SACLA. Journal of Physics: Conference Series, 2013, 425, 092009.	0.4	8
103	Femtosecond resonant magneto-optical Kerr effect measurement on an ultrathin magnetic film in a soft X-ray free electron laser. Japanese Journal of Applied Physics, 2018, 57, 09TD02.	1.5	8
104	Generation of an X-ray nanobeam of a free-electron laser using reflective optics with speckle interferometry. Journal of Synchrotron Radiation, 2020, 27, 883-889.	2.4	8
105	Protein–ligand complex structure from serial femtosecond crystallography using soaked thermolysin microcrystals and comparison with structures from synchrotron radiation. Acta Crystallographica Section D: Structural Biology, 2017, 73, 702-709.	2.3	8
106	Separating Non-linear Optical Signals of a Sample from High Harmonic Radiation in a Soft X-ray Free Electron Laser. E-Journal of Surface Science and Nanotechnology, 2022, 20, 31-35.	0.4	8
107	Hard x-ray intensity autocorrelation using direct two-photon absorption. Physical Review Research, 2022, 4, .	3.6	8
108	Generating 77 T using a portable pulse magnet for single-shot quantum beam experiments. Applied Physics Letters, 2022, 120, 142403.	3.3	8

#	Article	IF	CITATIONS
109	Damage study of optical substrates using 1-î¼m-focusing beam of hard X-ray free-electron laser. Journal of Physics: Conference Series, 2013, 463, 012043.	0.4	7
110	Real-time observation of disintegration processes within argon clusters ionized by a hard-x-ray pulse of moderate fluence. Physical Review A, 2020, 101, .	2.5	7
111	Characterizing the intrinsic properties of individual XFEL pulses via single-particle diffraction. Journal of Synchrotron Radiation, 2020, 27, 17-24.	2.4	7
112	Suppression of thermal nanoplasma emission in clusters strongly ionized by hard x-rays. Journal of Physics B: Atomic, Molecular and Optical Physics, 2021, 54, 044001.	1.5	7
113	Comparing the spatial coherence of the natural and focused X-rays from a free electron laser. Optics Express, 2019, 27, 19573.	3.4	7
114	Compact bolometric radiometer for free-electron lasers in a wavelength range from extreme-ultraviolet to x-rays. Optics Letters, 2017, 42, 4776.	3.3	7
115	Crystallization kinetics of atomic crystals revealed by a single-shot and single-particle X-ray diffraction experiment. Proceedings of the National Academy of Sciences of the United States of America, 2021, 118, .	7.1	7
116	Lipidic cubic phase serial femtosecond crystallography structure of a photosynthetic reaction centre. Acta Crystallographica Section D: Structural Biology, 2022, 78, 698-708.	2.3	7
117	Scanning magneto-optical Kerr effect (MOKE) measurement with element-selectivity by using a soft x-ray free-electron laser and an ellipsoidal mirror. Applied Physics Letters, 2020, 117, .	3.3	6
118	Refinement for single-nanoparticle structure determination from low-quality single-shot coherent diffraction data. IUCrJ, 2020, 7, 10-17.	2.2	6
119	Inducing thermodynamically blocked atomic ordering via strongly driven nonequilibrium kinetics. Science Advances, 2021, 7, eabj8552.	10.3	6
120	Excited-state intermediates in a designer protein encoding a phototrigger caught by an X-ray free-electron laser. Nature Chemistry, 2022, 14, 1054-1060.	13.6	6
121	Electron spectroscopic study of nanoplasma formation triggered by intense soft x-ray pulses. Journal of Chemical Physics, 2019, 151, 184305.	3.0	5
122	Multi-particle momentum correlations extracted using covariance methods on multiple-ionization of diiodomethane molecules by soft-X-ray free-electron laser pulses. Physical Chemistry Chemical Physics, 2020, 22, 2648-2659.	2.8	5
123	Ellipsometer Equipped with Multiple Mirrors for Element-selective Soft X-ray Experiments. E-Journal of Surface Science and Nanotechnology, 2020, 18, 231-234.	0.4	5
124	Absolute laser-intensity measurement and online monitor calibration using a calorimeter at a soft X-ray free-electron laser beamline in SACLA. Nuclear Instruments and Methods in Physics Research, Section A: Accelerators, Spectrometers, Detectors and Associated Equipment, 2018, 894, 107-110.	1.6	4
125	Structural Investigation of Single Specimens with a Femtosecond X-Ray Laser: Routes to Signal-to-Noise Ratio Enhancement. Physical Review Applied, 2020, 13, .	3.8	4
126	Single shot x-ray diffractometry in SACLA with pulsed magnetic fields up to 16 T. Physical Review Research, 2020, 2, .	3.6	4

#	Article	IF	CITATIONS
127	Characterizing crystalline defects in single nanoparticles from angular correlations of single-shot diffracted X-rays. IUCrJ, 2020, 7, 276-286.	2.2	4
128	An optical design of twin Wolter mirrors for focusing and imaging experiments with soft X-ray free electron lasers. , 2019, , .		4
129	Overview of optics, photon diagnostics and experimental instruments at SACLA: development, operation and scientific applications. , 2017, , .		3
130	Polarization control with an X-ray phase retarder for high-time-resolution pump–probe experiments at SACLA. Journal of Synchrotron Radiation, 2019, 26, 1139-1143.	2.4	3
131	Single-shot spectrometer using diamond microcrystals for X-ray free-electron laser pulses. Journal of Synchrotron Radiation, 2022, 29, 862-865.	2.4	3
132	Diverse Application Platform for Hard X-ray Diffraction in SACLA (DAPHNIS). Synchrotron Radiation News, 2017, 30, 12-15.	0.8	2
133	Multi-Beamline Operation Expands Research Opportunity at SACLA. Synchrotron Radiation News, 2017, 30, 11-16.	0.8	2
134	Microcrystal preparation for serial femtosecond X-ray crystallography of bacterial copper amine oxidase. Acta Crystallographica Section F, Structural Biology Communications, 2021, 77, 356-363.	0.8	2
135	Crystal structure of CmABCB1 multi-drug exporter in lipidic mesophase revealed by LCP-SFX. IUCrJ, 2022, 9, 134-145.	2.2	2
136	Evaluation of Pulse Duration of the Soft X-ray Free Electron Laser at SACLA BL1 with Single-Shot Spectrometry. , 2018, , .		0
137	XFEL Crystal Structures of Peroxidase Compound II. Angewandte Chemie, 2021, 133, 14699-14706.	2.0	0
138	An arrayed-window microfluidic device for observation of mixed nanoparticles with an X-ray free-electron laser. Optical Review, 2022, 29, 7.	2.0	0